3 Biotech (2019) 9:19
https://doi.org/10.1007/s13205-018-1559-6

ORIGINAL ARTICLE

High-yield expression in *Escherichia coli*, biophysical characterization, and biological evaluation of plant toxin gelonin

Guo-Bin Ding[1,2] · Gengfeng Wu[1,2] · Binchun Li[1] · Peng Yang[1,2] · Zhuoyu Li[1,2,3]

Received: 12 November 2018 / Accepted: 26 December 2018

Abstract
Gelonin is a plant toxin that exerts potent cytotoxic activity by inactivation of the 60S ribosomal subunit. The high-level expression of soluble gelonin still remains a great challenge and there was no detailed biophysical analysis of gelonin from *Escherichia coli* (*E. coli*) yet. In this study, the soluble and high-yield expression of recombinant gelonin (rGel) was achieved in *E. coli* BL21 (DE3) for the first time, with a yield of 6.03 mg/L medium. Circular dichroism (CD) analysis indicated that rGel consisted of 21.7% α-helix, 26.3% β-sheet, 18.5% β-turn, and 32.3% random coil, and it could maintain its secondary structure up to 60 °C. The antitumor activity of rGel was evaluated in two colon cancer cell lines—HCT116 and HCT-8, and it was clearly demonstrated that rGel exerted antiproliferative activity against these two cell lines by inhibiting cellular protein synthesis. These findings provide insights for researchers involved in the expression of similar biotoxins, and the biophysical characterizations of gelonin will favor its further therapeutic applications.

Keywords Gelonin · High-yield expression · Biophysical characterization · *E. coli* · Biological evaluation

Introduction

Depending on the type of cancer, its location and stage, and the physical condition of the patients, different cancer treatment modalities (including surgery, chemotherapy, radiation therapy, targeted therapy, and immunotherapy) or a combination of them can be employed (Turek et al. 2016). As a standard treatment for cancer, current chemotherapy mainly relies on small-molecule agents, and most of them suffered from low efficacy and severe side effects (Ding et al. 2012, 2014, 2018a; Ye et al. 2015). Given the ineffectiveness of small-molecule chemotherapeutic agents, macromolecular drugs have attracted growing interest over the past few decades because of their unparalleled potency and unique mode of action (Ye et al. 2015). One representative example is the plant-derived ribosome-inactivating proteins (RIPs), which exhibits a glycosidase activity and can be classified into three groups referred to as types I, II, and III (Chang et al. 2017). Type I RIPs consist of a single polypeptide chain (A-chain) with catalytic activity, type II RIPs are heterodimeric glycoproteins composed of an A-chain (similar to type I RIPs) linked to a B chain (mediating cellular internalization) via disulfide bond. Type III RIPs comprise an A-chain and an additional protein fragment that requires a proteolytic cleavage to give active RIPs (Stirpe 2013; Chang et al. 2017). RIPs hold great potential for biomedical applications due to their various biological activities such as antiviral, antiparasitic, and anticancer properties (Stirpe 2006).

Gelonin, a type I RIP, is a plant toxin originally isolated from the seeds of *Gelonium multiflorum* (Daubenfeld et al. 2005). It can induce the irreversible inactivation of ribosomes via cleaving the adenine 4324 of the eukaryotic 28S ribosomal RNA, and thereby inhibiting protein synthesis (Hossann et al. 2006). Gelonin has drawn extensive interest in recent years, since many investigations demonstrated

Electronic supplementary material The online version of this article (https://doi.org/10.1007/s13205-018-1559-6) contains supplementary material, which is available to authorized users.

✉ Guo-Bin Ding
dinggb2012@sxu.edu.cn

✉ Zhuoyu Li
lzy@sxu.edu.cn

1 Institute of Biotechnology, The Key Laboratory of Chemical Biology and Molecular Engineering of Ministry of Education, Shanxi University, Taiyuan 030006, China

2 Institutes of Biomedical Sciences, Shanxi University, Taiyuan 030006, China

3 School of Life Science, Shanxi University, Taiyuan 030006, China

Published online: 02 January 2019

that it exhibited an excellent performance for the treatment of a variety of diseases such as malaria, AIDS, and cancer via different mechanisms (Woodhams et al. 2010). Unfortunately, the poor cellular uptake, low yield of extraction and heterogeneous expression, and limited information on its biophysical characteristics greatly hinder its clinical application (Stirpe et al. 1980; Bai et al. 2015; Shin et al. 2015). Although it has been reported that type I RIPs are able to enter some mammalian cells (Puri et al. 2012; Bolognesi et al. 2016), most of the current reports focused on improving the cellular internalization of gelonin via integration of targeting ligands by chemical conjugation or expressing a fusion gelonin protein. A broad variety of targeting molecules, including anti-insulin-like growth factor-1 receptor (IGF-1R) affibody (IAFF) (Ham et al. 2017), cell penetrating peptide (CPP) (Shin et al. 2013, 2014), melittin (Shin et al. 2016), the tenth human fibronectin type III domain (Fn3) (Pirie et al. 2013), and epidermal growth factor (EGF) (Berstad et al. 2015), have been attached to gelonin to enhance its cellular uptake and antitumor efficiency. More recently, extracellular vesicle membrane (EVM)-camouflaged metal–organic framework (MOF) nanoparticles were designed and fabricated for systemic and intracellular delivery of gelonin (Cheng et al. 2018). However, to the best of our knowledge, there have been no previous reports on the high-yield soluble expression and detailed biophysical characterization of gelonin despite they are also of great importance for its therapeutic application.

In the present study, we report the soluble and high-yield expression of recombinant gelonin (rGel) in *E. coli*, and the purified rGel was analyzed by sodium dodecyl sulfate polyacrylamide gel electrophoresis (SDS-PAGE) and matrix-assisted laser desorption ionization time-of-flight mass spectrometry (MALDI-TOF-MS). The secondary structure and thermal stability of rGel were investigated in detail by CD. Finally, we determined the in vitro antitumor activity of rGel against two colon cancer cell lines and uncovered the underlying mechanism.

Materials and methods

Materials

TransStart FastPfu Fly DNA polymerase, EasyPfu DNA polymerase, Trans2K Plus II DNA Marker, Blue Plus II Protein Marker, competent *E. coli* DH5α, and *E. coli* BL21 (DE3) strains were supplied by TransGen Biotech Co., Ltd (China). pET28a-*pHLIP-Gelonin* plasmid was constructed by our group. Kanamycin, isopropyl β-D-1-thiogalactopyranoside (IPTG), and imidazole were obtained from Beijing Gentihold Biotechnology Co. Ltd (China). Ni-nitrilotriacetic acid (NTA) resin was purchased from Beijing Biodragon Immunotechnologies Co., Ltd (China). Bicinchoninic acid (BCA) assay kit was provided by Beyotime Institute of Biotechnology (China). 3-(4,5-Dimethylthiazol-2-yl)-2,5-diphenyltetrazolium bromide (MTT) was purchased from Sigma-Aldrich.

Construction of recombinant expression vector pET28a-*Gelonin*

The recombinant expression vector pET28a-*Gelonin* was obtained by whole plasmid polymerase chain reaction (PCR), using pET28a-*pHLIP-Gelonin* as the template. The primer sequence used for whole plasmid PCR were as follows: forward primer: 5′-ATATACCATGGGCCTGGATAC CGTGAGCTTCAGC-3′; the reverse primer: 5′-GTATCC AGGCCCATGGTATATCTCCTTCTTAAAG-3′. The volume of PCR reaction system was 50 µL containing ddH_2O, TransStart FastPfu Fly buffer, dNTPs, primers, TransStart FastPfu Fly DNA polymerase, and DNA template. PCR procedures utilized were shown as follows: denaturation at 95 °C for 5 min, 20 cycles at 95 °C for 30 s, 55 °C for 30 s, 72 °C for 3.5 min, then 72 °C for 30 min, and 12 °C for 2–3 h.

Expression of recombinant gelonin (rGel) in *E. coli*

Recombinant plasmid pET28a-*Gelonin* was transformed into competent *E. coli* BL21 (DE3) cells. A single colony harboring the pET28a-*Gelonin* recombinant plasmid was isolated and inoculated into 5 mL Luria–Bertani (LB) medium-containing 50 µg/mL kanamycin, which was incubated in a shaker for 8 h (37 °C, 200 rpm). Then, the culture was transferred into 400 mL fresh LB medium-containing 50 µg/mL kanamycin and incubated at the same condition until reaching an OD600 of 0.6–0.8. Protein expression was triggered by adding the inducer isopropyl β-D-1-thiogalactopyranoside (IPTG) at a final concentration of 0.5 mM, and the culture was further incubated in a shaker (37 °C, 180 rpm) for 12 h. The cells were collected by centrifugation (8000 rpm, 10 min), resuspended in 20 mM Tris (150 mM NaCl, pH 8.0), and lysed by sonication on ice. Finally, the cells were centrifuged at 12,000 rpm for 30 min at 4 °C, and both the soluble (supernatant) and insoluble (cell pellet) fractions were collected and analyzed by SDS-PAGE.

Purification of rGel

Cell-free supernatant-containing soluble rGel was collected and loaded onto Ni–NTA resins (Beijing Biodragon Immunotechnologies Co., Ltd, China). The resins were washed with 80 mM imidazole (20 mM Tris, 150 mM NaCl, pH 8.0) to remove the unbound proteins. And the rGel was acquired after elution with 400 mM imidazole (20 mM Tris, 150 mM

NaCl, pH 8.0). The obtained rGel solution was concentrated and desalted using an ultrafiltration membrane (Millipore, 10 kDa, USA) for several times. The purity of rGel was evaluated by densitometry analysis of the observed band at 29 kDa from SDS-PAGE results using ImageJ software, while the production yield was determined via BCA assay.

MALDI-TOF-MS analysis of rGel

The purified rGel was subjected to SDS-PAGE analysis; the band at 29 kDa was cut out and put into a 1.5 mL tube. MALDI-TOF-MS analysis was performed by Sangon Biotech Co., Ltd. (Shanghai, China). Both the MS and MS/MS data were integrated and processed by the GPS Explorer V3.6 software (Applied Biosystems, USA) and Mascot V2.3 search engine (Matrix Science Ltd., London, UK).

Biophysical characterization of rGel

The CD spectra of purified rGel (6 μM) at different temperatures (20, 30, 40, 50, 60, 70, 80, 90, and 98 °C) were recorded in a range of 190–260 nm on a temperature-controlled Chirascan spectrometer (Applied Photophysics, UK) with a heating rate of 1 °C/min, and the scanning speed is 1 nm/s. And the content of secondary structures was calculated via CDNN software. Deconvolution of the CD data was conducted in the range of 190–260 nm. In deconvolution process, the essential parameters were input as follows: molecular mass: 29,319 Da, concentration: 0.176 mg/mL, number of amino acids: 260, and pathlength: 0.1 cm.

Cytotoxicity of rGel

HCT116 and HCT-8 cells were seeded into 96-well plates at a density of 5×10^3 cells per well and incubated overnight in RPMI-1640 medium-containing 10% fetal bovine serum (FBS) at 37 °C. The medium was removed and fresh medium-containing various concentrations (10^{-9}, 10^{-8}, 10^{-7}, 10^{-6}, and 10^{-5} M) rGel was added. After incubation for 48 or 72 h, the medium was replaced by 100 μL serum-free fresh RPMI-1640 and 20 μL MTT solution (5 mg/mL in PBS), and incubated for another 4 h. Finally, 150 μL of dimethyl sulfoxide (DMSO) was added into each well and the absorbance at 570 nm was recorded on a microplate reader.

Cellular protein synthesis inhibition assay

The inhibitory effect of rGel on cellular protein synthesis was determined according to a previous report (Shin et al. 2016). Briefly, HCT116 and HCT-8 cell were seeded into 12-well plates at a density of 1×10^5 cells per well and allowed to attach to the bottom of plates overnight in RPMI-1640 medium-containing 10% FBS at 37 °C. Then, the cells were treated with various concentrations (10^{-9}, 10^{-8}, 10^{-7}, 10^{-6}, and 10^{-5} M) of rGel for 48 or 72 h. The medium was removed and cells were washed twice with PBS, and 1% triton X-100 was added to lyse cells. Cell lysates were harvested and centrifuged at 12,000 rpm for 15 min. The protein content in the supernatant was determined by BCA protein assay and the relative cellular protein levels were calculated as the ratio of protein contents in treated groups to those of control groups.

Statistical analysis

All data are presented as the mean ± SD (standard deviations). Statistical analysis between two groups was conducted using a two-tailed Student's *t* test. The differences were considered statistically significant when $P < 0.05$ and highly significant when $P < 0.01$.

Results and discussion

Expression and purification of rGel

Notwithstanding numerous reports on the potent antitumor efficacy of gelonin, its provision is far from sufficient particularly due to an increasing demand for preclinical investigation. The amount of *G. multiflorum* seeds is limited, and the complicated extraction and multistep purification processes compromise the yield of gelonin (Ajji et al. 2018). Expression of recombinant proteins in microbial systems provides an alternative strategy to obtain recombinant gelonin (rGel). *Escherichia coli* is one of the most popular microorganisms and a well-established cell factory for the production of heterologous proteins (Rosano and Ceccarelli 2014), and the *E. coli* BL21 pET expression system has become one of the most commonly used ones for cloning and expression of recombinant proteins (Mohammadzadeh et al. 2017). Recently, we successfully overexpressed a soluble and functional fusion protein (Trx-pHLIP-Beclin 1, TpB) in *E. coli* BL21 (DE3) with a high yield of 21.9 mg/L (Ding et al. 2018b).

Whole plasmid PCR was employed to obtain the recombinant plasmid pET28a-*Gelonin*, and pET28a-*pHLIP-Gelonin* was used as the template. The successful construction of pET28a-*Gelonin* and its transformation into *E. coli* DH5α were verified by agarose gel electrophoresis (Fig. S1). In addition, the positive colony was subjected to DNA sequencing, the nucleotide sequence of the pET28a-*Gelonin* was completely correct and no mutation was observed (data not shown), indicating that the recombinant expression vector was successfully constructed.

For expression of recombinant gelonin (rGel), pET28a-*Gelonin* was transformed into *E. coli* BL21 (DE3) and cultured in LB medium-containing 50 µg/mL kanamycin. The rGel expression was initiated by addition of IPTG with a final concentration of 0.5 mM and incubated at 37 °C for 12 h. Total cell extract, the supernatant, and pellet fraction of cell lysate of *E. coli* BL21 (DE3) were harvested and analyzed via SDS-PAGE. An intense band at about 29 kDa (Fig. 1a, lane 2 and 3) was observed in the total cell extract and supernatant after IPTG induction, while no band at this position was visible in the cell pellet (Fig. 1a, lane 4), indicating rGel was overexpressed in a soluble form. As expected, there is no rGel expression in *E. coli* BL21 (DE3) harboring empty pET28a plasmid and *E. coli* BL21 (DE3) without IPTG induction (Fig. 1a, lane 1 and 5).

There is a C-terminal 6 × His tag in rGel, and thus, it is purified by a Ni–NTA metal affinity column chromatography. The purified rGel was eluted from the column by 400 mM imidazole after washing with 80 mM imidazole to remove unbound proteins. As presented in Fig. 1b, only one strong band at about 29 kDa can be seen on the SDS-PAGE after purification. The purity of the purified rGel is about 95% as determined by the densitometry analysis of the SDS-PAGE gels using imageJ software. Moreover, the average yield of the purified rGel was 6.03 mg per liter LB medium as measured by BCA assay, which is approximately five times higher than the previous reports (1 mg/L) (Shin et al. 2013, 2015).

MALDI-TOF mass spectrometry analysis of rGel

Currently, matrix-assisted laser desorption ionization time-of-flight mass spectrometry (MALDI-TOF-MS) has become one of the most widely used tools for the rapid and sensitive analysis of biomolecules including proteins (Counterman et al. 2003). The molecular weight of rGel determined by MALDI-TOF-MS is 29,319 Da, which matches well with the theoretical value (29.23 kDa). The purified rGel was subjected to tryptic digestion and the obtained peptide fragments were analyzed by MALDI-TOF-MS. The acquired peptide masses were identified using the Mascot V2.3 search engine with a precursor ion tolerance of 100 and a fragment ion tolerance of 0.3 Da. As shown in Fig. 2, a series of peptides with 936.4855–3459.7551 Da were detected. Ten independent peptide fragments matched the predicted sequence for a 259 amino acid protein, as shown in Table 1, and the sequence coverage was 47%, indicating the successful and correct expression of rGel.

Biophysical analysis of rGel

Circular dichroism (CD) is a convenient method for rapid analysis of the secondary structure and environmentally induced structural changes of recombinant proteins and proteins isolated from various organisms (Greenfield 2006; Li et al. 2011; Wei et al. 2014). The secondary structure of rGel was determined by CD at 25 °C and the spectrum is shown in Fig. 3a. CDNN (version 2.1) is a deconvolution software which can be used to quantify the content of different secondary structures in the far UV region of

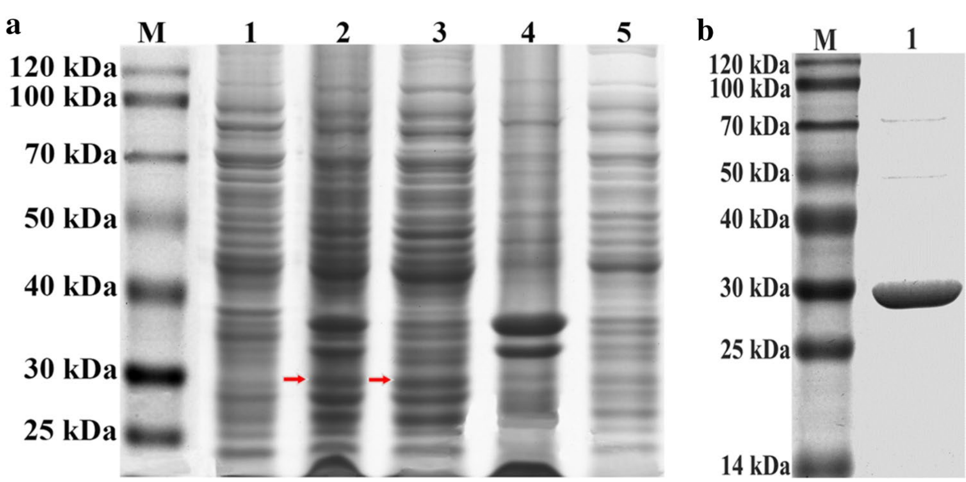

Fig. 1 **a** SDS-PAGE analysis of recombinant gelonin (rGel) expression. Lane M: protein molecular weight markers; Lane 1: the supernatant of cell lysate of *E. coli* BL21 (DE3) harboring empty pET28a plasmid with IPTG induction; Lanes 2, 3, 4: total cell extract, the supernatant and pellet fraction of cell lysate of *E. coli* BL21 (DE3) harboring pET28a-*Gelonin* plasmid with IPTG induction. Lane 5: the supernatant of cell lysate of *E. coli* BL21 (DE3) harboring pET28a-*Gelonin* plasmid without IPTG induction. The red arrows indicate the target protein. **b** SDS-PAGE of rGel after purification by nickel affinity column chromatography. Lane M: protein molecular weight marker; lane 1: purified rGel

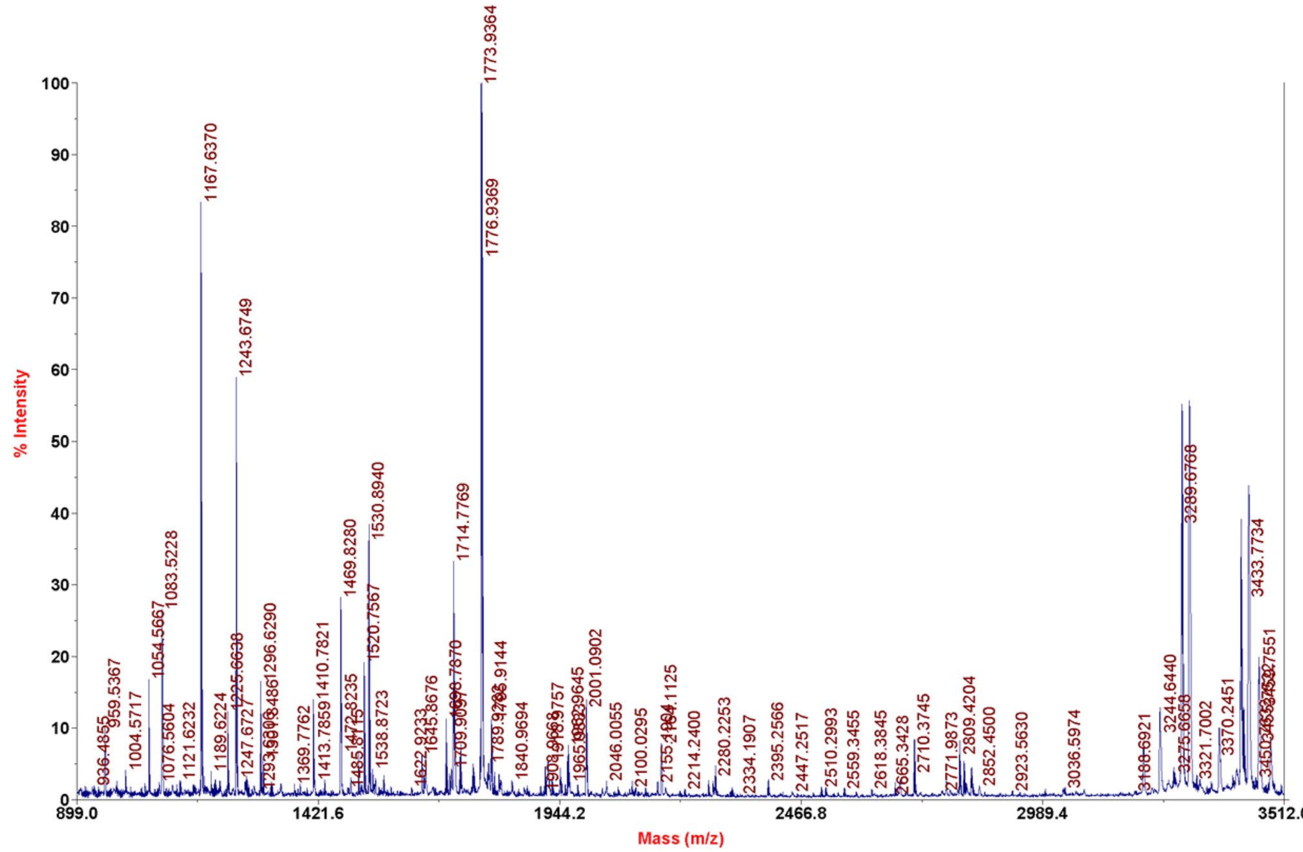

Fig. 2 MALDI-TOF mass spectrum of purified rGel after tryptic digestion

Table 1 Peptide mass fingerprinting analysis of purified rGel by MALDI-TOF mass spectrometry

Peptides	Position	Observed	Calculated
-.GLDTVSFSTK.G	1–10	1054.5669	1053.5343
K.GATYITYVNFLNELR.V	11–25	1773.9358	1772.9097
K.LKPEGNSHGIPLLR.K	28–41	1530.8940	1529.8678
K.DAPDAAYEGLFK.N	89–100	1296.6293	1295.6034
R.LHFGGSYPSLEGEK.A	107–120	1520.7567	1519.7307
R.ETTDLGIEPLR.I	124–134	1243.6749	1242.6456
R.FTFIENQIR.N	170–178	1167.6370	1166.6084
R.IRPANNTISLENK.W	185–197	1469.8280	1468.7997
R.TSGANGMFSEAVELER.A	207–222	1713.7874	1712.7675
K.LEHHHHHH.-	252–259	1083.5220	1082.4907

CD spectra (Ioannou et al. 2015). The content of various secondary structures of rGel was calculated via CDNN software, and it contains 21.7% α-helix, 26.3% β-sheet (both parallel and antiparallel), 18.5% β-turn, and 32.3% random coil. Obviously, β-sheet and random coils are the predominant secondary structures of rGel. This is different from one previous report based on Raman spectroscopy (Pal and Bajpai 1998), possibly due to the different measurement methods and different origins of gelonin.

As can be seen from Fig. 3b, the CD spectra of rGel from 20 to 60 °C are almost completely superimposed, indicating the high thermal stability of rGel in this temperature range. However, we can observe an obvious variation in the CD spectra above 60 °C, suggesting that rGel is unstable at higher temperatures (70–98 °C). The calculated secondary structure values of rGel in the range of 20–98 °C are presented in Table 2. There are only some slight fluctuations in secondary structure contents at 20–60 °C as calculated by CDNN. It is apparent that there is a slight increase in α-helix, a negligible decrease in the β-turn, and a marked increase in random coils in 70–98 °C. This pattern of thermal stability of rGel was consistent with the previous report (Pal and Bajpai 1998), indicating that rGel has a similar thermal stability with the isolated gelonin.

In vitro antitumor activity of rGel

As demonstrated in numerous previous studies, gelonin displayed an excellent antitumor efficacy against a variety of cancers. In addition, it has been assumed that a single gelonin suffices to destroy one cancer cell if it could gain

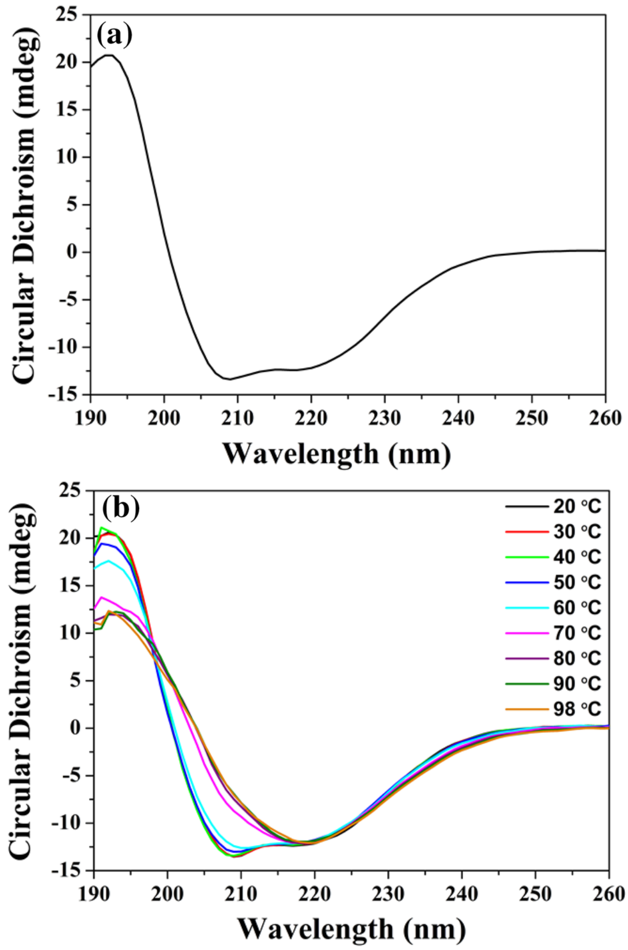

Fig. 3 **a** CD spectrum of purified rGel (6 μM) at 25 °C; **b** CD spectra of purified rGel (6 μM) at a wide range of temperatures (20–98 °C)

access to the ribosome (Shin et al. 2013). Therefore, we determined the cytotoxicity of rGel against two colon cancer cells—HCT116 and HCT-8—by MTT assay. As presented in Fig. 4, rGel exerted a dose- and time-dependent inhibitory effect on the growth of both HCT116 and HCT-8 cells. The highest inhibitory rates of rGel against HCT116 and HCT-8 were 52.50% and 44.31%, respectively, after exposure to 10 μM rGel for 72 h (Fig. 4). However, the prominent antitumor effect of rGel can only be observed at higher concentrations (micromolar level), which is consistent with the previous reports (Shin et al. 2013, 2014, 2015, 2016). These results clearly indicated the low efficacy of rGel cellular internalization possibly via fluid phase endocytosis. Thus, it is necessary to remarkably enhance the cellular uptake of gelonin by conjugating some targeting moieties to it.

Suppression of cellular protein synthesis

Since the antitumor efficiency of gelonin is attributed to its intrinsic N-glycosidase activity, we examined whether rGel still retains this activity. After treatment of HCT116 and HCT-8 cells with different concentrations of rGel for 48 and 72 h, the cells were harvested and lysed, and the cellular protein level was determined via BCA assay. As shown in Fig. 5, rGel inhibited the cellular protein synthesis in both tested cells in a concentration- and time-dependent manner. Consistent with MTT results, only the micromolar level rGel exhibited a significant suppression on protein synthesis. And the relative cellular protein levels in HCT116 and HCT-8 cells were 14.56% and 35.62% of control cells, respectively, after incubation with 10 μM rGel for 72 h (Fig. 5). These results suggest that the underlying mechanism of the in vitro antitumor effect of rGel can be ascribed to its glycosidase activity.

Conclusion

In conclusion, this is the first report on the high-yield and soluble expression of gelonin in *E. coli*. Under suitable conditions (37 °C, 0.5 mM IPTG and an induction time of 12 h), the high-level and reproducible production of gelonin in *E. coli* was achieved, and the yield is about 6.03 mg/L. The introduction of a His tag on the C-terminus of the protein facilitated purification of gelonin by nickel affinity

Table 2 Secondary structure contents of purified rGel (6 μM) at different temperatures (20–98 °C) as calculated by CDNN software

	Helix (%)	Antiparallel (%)	Parallel (%)	Beta-turn (%)	Random coil (%)	Total sum (%)
20 °C	21.7	20.4	5.9	18.4	32.5	98.9
30 °C	21.5	20.9	5.8	18.6	32.2	99.0
40 °C	21.4	20.8	5.8	18.6	32.3	98.9
50 °C	21.1	21.5	5.8	18.6	32.4	99.4
60 °C	20.9	21.9	5.8	18.6	32.9	100.1
70 °C	22.0	19.8	6.3	17.6	37.2	102.9
80 °C	22.4	18.8	6.5	17.2	39.0	103.9
90 °C	22.4	18.8	6.5	17.1	39.1	104.0
98 °C	22.7	17.9	6.6	16.9	40.0	104.1

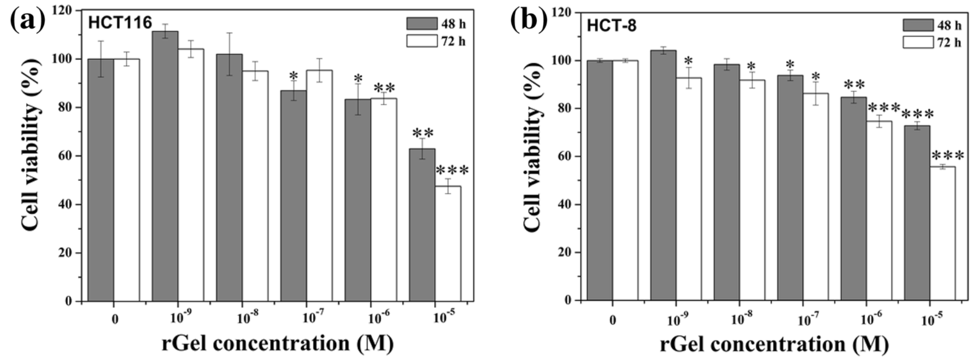

Fig. 4 In vitro cytotoxicity assay of rGel. HCT116 (**a**) and HCT-8 (**b**) cells were exposed to rGel of various concentrations (0–10^{-5} M) for 48 h and 72 h, and cell viability was analyzed by MTT assay. *Indicates $P<0.05$, **indicates $P<0.01$, and ***indicates $P<0.001$ as compared to control

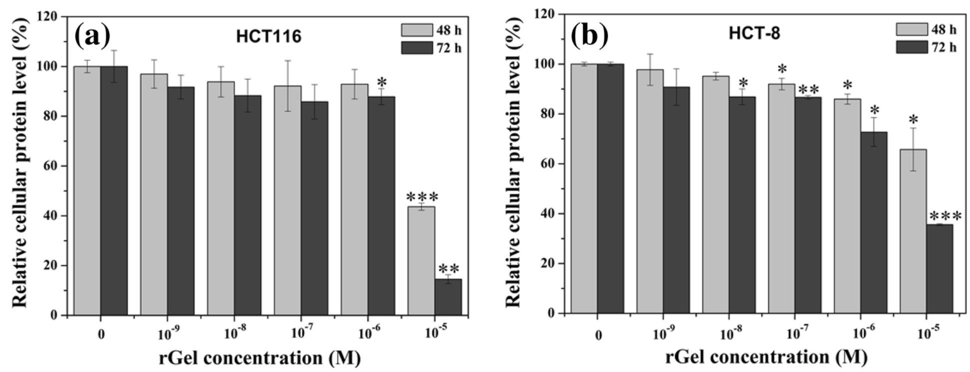

Fig. 5 HCT116 (**a**) and HCT-8 (**b**) cells were incubated with various concentrations (0–10^{-5} M) of rGel for 48 h and 72 h, and the relative cellular protein level was determined by BCA assay. *Indicates $P<0.05$, **indicates $P<0.01$, and ***indicates $P<0.001$ as compared to control

chromatography. Analysis of secondary structure revealed that recombinant gelonin was mainly composed of β-sheet and random coil. It was found that rGel was thermostable and could retain its structure in the range of 20–60 °C. In vitro antitumor assays showed that gelonin could inhibit the proliferation of two colon cancer cells in a dose- and time-dependent manner via suppressing the protein synthesis. This study not only provides a feasible and effective approach for high-level production of plant-derived toxin gelonin, but also enables further investigation into the mechanism of its antitumor efficacy.

Acknowledgements This study was supported by the National Natural Science Foundation of China (No. 31500771) and "1331 Project" Key Innovation Team of Shanxi Province (Prof. Zhuoyu Li). The authors would like to thank Dr. Yaoming Liu from Scientific Instrument Center of Shanxi University for his helpful discussion in CD characterizations.

Compliance with ethical standards

Conflict of interest The authors declare no conflict of interests.

References

Ajji PK, Sonkar SP, Walder K, Puri M (2018) Purification and functional characterization of recombinant balsamin, a ribosome-inactivating protein from *Momordica balsamina*. Int J Biol Macromol 114:226–234

Bai Y, Gou M, Yi T, Yang L, Liu L, Lin X, Su D, Wei Y, Zhao X (2015) Efficient inhibition of ovarian cancer by gelonin toxin gene delivered by biodegradable cationic heparin-polyethyleneimine nanogels. Int J Med Sci 12:397–406

Berstad MB, Cheung LH, Berg K, Peng Q, Fremstedal AS, Patzke S, Rosenblum MG, Weyergang A (2015) Design of an EGFR-targeting toxin for photochemical delivery: in vitro and in vivo selectivity and efficacy. Oncogene 34:5582–5592

Bolognesi A, Bortolotti M, Maiello S, Battelli MG, Polito L (2016) Ribosome-inactivating proteins from plants: a historical overview. Molecules 21:1627

Chang CD, Lin PY, Chen YC, Huang HH, Shih WL (2017) Novel purification method and antibiotic activity of recombinant *Momordica charantia* MAP30. 3 Biotech 7(3):3

Cheng G, Li W, Ha L, Han X, Hao S, Wan Y, Wang Z, Dong F, Zou X, Mao Y, Zheng SY (2018) Self-assembly of extracellular vesicle-like metal-organic framework nanoparticles for protection and intracellular delivery of biofunctional proteins. J Am Chem Soc 140:7282–7291

Counterman AE, Thompson MS, Clemmer DE (2003) Identifying a protein by MALDI-TOF mass spectrometry: an experiment for the undergraduate laboratory. J Chem Educ 80:177–180

Daubenfeld T, Hossann M, Trommer WE, Niedner-Schatteburg G (2005) On the contentious sequence and glycosylation motif of the ribosome inactivating plant protein gelonin. Biochem Biophys Res Commun 333:984–989

Ding GB, Liu HY, Lv YY, Liu XF, Guo Y, Sun CK, Xu L (2012) Enhanced in vitro antitumor efficacy and strong anti-cell-migration activity of a hydroxycamptothecin-encapsulated magnetic nanovehicle. Chem A Eur J 18:14037–14046

Ding GB, Wang Y, Guo Y, Xu L (2014) Integrin $\alpha_v\beta_3$-targeted magnetic nanohybrids with enhanced antitumor efficacy, cell cycle

arrest ability, and encouraging anti-cell-migration activity. ACS Appl Mater Interfaces 6:16643–16652
Ding GB, Sun J, Yang P, Li B, Gao Y, Li Z (2018a) A novel doxorubicin prodrug with GRP78 recognition and nucleus-targeting ability for safe and effective cancer therapy. Mol Pharm 15:238–246
Ding GB, Sun J, Wu G, Li B, Yang P, Li Z, Nie G (2018b) Robust anticancer efficacy of a biologically synthesized tumor acidity-responsive and autophagy-inducing functional beclin 1. ACS Appl Mater Interfaces 10:5227–5239
Greenfield NJ (2006) Using circular dichroism spectra to estimate protein secondary structure. Nat Protoc 1:2876–2890
Ham S, Min KA, Yang JW, Shin MC (2017) Fusion of gelonin and anti-insulin-like growth factor-1 receptor (IGF-1R) affibody for enhanced brain cancer therapy. Arch Pharm Res 40:1094–1104
Hossann M, Li Z, Shi Y, Kreilinger U, Büttner J, Vogel PD, Yuan J, Wise JG, Trommer WE (2006) Novel immunotoxin: a fusion protein consisting of gelonin and an acetylcholine receptor fragment as a potential immunotherapeutic agent for the treatment of *Myasthenia gravis*. Protein Expr Purif 46:73–84
Ioannou JC, Donald AM, Tromp RH (2015) Characterising the secondary structure changes occurring in high density systems of BLG dissolved in aqueous pH 3 buffer. Food Hydrocoll 46:216–225
Li CH, Nguyen X, Narhi L, Chemmalil L, Towers E, Muzammil S, Gabrielson J, Jiang Y (2011) Applications of circular dichroism (CD) for structural analysis of proteins: qualification of near- and far-UV CD for protein higher order structural analysis. J Pharm Sci 100:4642–4654
Mohammadzadeh R, Agheshlouie M, Mahdavinia GR (2017) Expression of chitinase gene in BL21 pET system and investigating the biocatalystic performance of chitinase-loaded AlgSep nanocomposite beads. Int J Biol Macromol 104:1664–1671
Pal B, Bajpai PK (1998) Spectroscopic characterization of gelonin—assignments secondary structure and thermal denaturation. Indian J Biochem Biophys 35:166–171
Pirie CM, Liu DV, Wittrup KD (2013) Targeted cytolysins synergistically potentiate cytoplasmic delivery of gelonin immunotoxin. Mol Cancer Ther 12:1774–1782
Puri M, Kaur I, Perugini MA, Gupta RC (2012) Ribosome-inactivating proteins: current status and biomedical applications. Drug Discov Today 17:774–783
Rosano GL, Ceccarelli EA (2014) Recombinant protein expression in *Escherichia coli*: advances and challenges. Front Microbiol 5:172
Shin MC, Zhang J, David AE, Trommer WE, Kwon YM, Min KA, Kim JH, Yang VC (2013) Chemically and biologically synthesized CPP-modified gelonin for enhanced anti-tumor activity. J Controlled Release 172:169–178
Shin MC, Zhang J, Min KA, Lee K, Moon C, Balthasar JP, Yang VC (2014) Combination of antibody targeting and PTD-mediated intracellular toxin delivery for colorectal cancer therapy. J Controlled Release 194:197–210
Shin MC, Zhao J, Zhang J, Huang Y, He H, Wang M, Min KA, Yang VC (2015) Recombinant TAT–gelonin fusion toxin: synthesis and characterization of heparin/protamine-regulated cell transduction. J Biomed Mater Res Part A 103:409–419
Shin MC, Min KA, Cheong H, Moon C, Huang Y, He H, Yang VC (2016) Preparation and characterization of gelonin–melittin fusion biotoxin for synergistically enhanced anti-tumor activity. Pharm Res 33:2218–2228
Stirpe F (2006) Ribosome-inactivating proteins: progress and problems. Cell Mol Life Sci 63:1850–1866
Stirpe F (2013) Ribosome-inactivating proteins: from toxins to useful proteins. Toxicon 67:12–16
Stirpe F, Olsnes S, Pihl A (1980) Gelonin, a new inhibitor of protein synthesis, nontoxic to intact cells. J Biol Chem 255:6947–6953
Turek M, Krzyczmonik M, Balczewski P (2016) New hopes in cancer battle—a review of new molecules and treatment strategies. Med Chem 12:700–719
Wei Y, Thyparambil AA, Latour RA (2014) Protein helical structure determination using CD spectroscopy for solutions with strong background absorbance from 190 to 230 nm. Biochim Biophys Acta Proteins Proteom 1844:2331–2337
Woodhams J, Lou PJ, Selbo PK, Mosse A, Oukrif D, MacRobert A, Novelli M, Peng Q, Berg K, Bown SG (2010) Intracellular relocalisation by photochemical internalisation enhances the cytotoxic effect of gelonin—quantitative studies in normal rat liver. J Controlled Release 142:347–353
Ye J, Shin MC, Liang Q, He H, Yang VC (2015) 15 years of ATTEMPTS: a macromolecular drug delivery system based on the CPP-mediated intracellular drug delivery and antibody targeting. J Controlled Release 205:58–69